ACS APPLIED MATERIALS & INTERFACES

Applications of Polymer, Composite, and Coating Materials

Preparation of Gas-Responsive Imprinting Hydrogel and Their Gas Driven Switchable Affinity for Target Protein Recognition

Yubo Wei, Qiang Zeng, Jianzhi Huang, Xinrong Guo, Lulu Wang, and Lishi Wang

ACS Appl. Mater. Interfaces, **Just Accepted Manuscript** • DOI: 10.1021/acsami.0c05561 • Publication Date (Web): 04 May 2020

is published by the American Chemical Society. 1155 Sixteenth Street N.W., Washington, DC 20036

Preparation of Gas-Responsive Imprinting Hydrogel and Their Gas Driven Switchable Affinity for Target Protein Recognition

Yubo Wei[b], Qiang Zeng[a], Jianzhi Huang[a], Xinrong Guo[a], Lulu Wang[a], Lishi Wang[a*]

[a] Key Laboratory of Functional Molecular Engineering of Guangdong Province, School of Chemistry and Chemical Engineering, South China University of Technology, Guangzhou 510641, People's Republic of China

[b] School of Pharmaceutical Sciences and Yunnan Key Laboratory of Pharmacology for Natural Products, Kunming Medical University, Kunming, Yunnan 650500, People's Republic of China

*Corresponding author

Email: wanglsh@scut.edu.cn

Abstract

Novel gas-responsive imprinting hydrogel were fabricated by combining *N,N′*-dimethylaminoethyl methacrylate (DMAEMA) gas-sensitive monomer, *N,N′*-methylenebis(acrylamide) (MBAAm) cross-linker and human serum albumin (HSA) template proteins via a free radical polymerization. The hydrogel exhibited a reversible gas-responsive property upon N_2/CO_2 exchange. This result was supported by the evidences from hydrogen nuclear magnetic resonance spectroscopy (^{1}H NMR) and scanning electron microscopy (SEM). By applying this property to sensing application, a CO_2-responsive imprinted biosensor was originally designed on the surface of a glassy carbon electrode (GCE). The biosensor exhibited unique self-clean and self-recognition properties toward HSA proteins basing on reversible conformational changes driven by N_2/CO_2 stimuli. Moreover, the proposed imprinted biosensor favored HSA proteins by showing satisfying sensitivity and selectivity and a wider detection range with a low detection limit. As a rare example in imprinting sensing, the biosensor was successfully applied to the HSA extraction from complex serum samples. With gas stimuli, the whole process was efficient, controllable, and harmless to the proteins. Thus, the developed biosensor may provide a new prospect

in molecularly imprinted sensing applications.

Keywords: stimuli-responsive polymers; molecular imprinting hydrogel; gas-responsive materials; protein recognition; biosensor

Introduction

Macromolecular stimuli-responsive polymers have been defined as "smart" materials, which can sense external stimulating signals (*e.g.* temperature,[1-5] enzyme concentration,[6] pH,[7] light,[8-11] electric,[12] and magnetic field[13]) and respond by performing considerable changes in their physical or chemical properties. Thus, stimuli-responsive polymers have arisen growing attention, owing to their potential applications in biotechnology,[14] functional materials,[15, 16] chemosensors,[17] separation sciences,[18] and nanomedicine.[19, 20] In particular, stimuli-responsive polymers combining with molecular imprinting technology can achieve intelligent mimicking with the natural receptors' properties. The resulting stimuli-responsive molecularly imprinted polymers (SR-MIPs) can also overcome some shortcomings of common MIPs like self-eluting template molecules and maintain the stability of structures within the imprinted process.[21-28] As reported recently, polymers based on thermo-responsive hydrogel show self-cleaning property toward imprinted bovine serum albumin (BSA) at 37 °C.[1] Additionally, taking advantage of the reductive generation of hydrogen from the electrolysis of water under an electric field stimulus, we prepared an electro-responsive imprinted biosensor to achieve the purpose of rapid elution template protein under an electric field trigger.[29]

In view of the above advantages, pH-responsive polymers are by contrast the most applied cases and have achieved huge commercial and academic values due to the proton acceptor and donor abilities of contained ionisable acidic or basic residues.[30-33] This property allows pH-responsive polymers to tune their conformations, hydrophobic/hydrophilic properties, and swelling/deswelling states *etc.*, by the change of hydrodynamic volume in polymer chains. However, reversible stimulus responsiveness of pH-responsive polymers is commonly triggered by the extra introduced acids and bases. The added chemical reagents results that the process

cycles are accompanied by the formation of a large number of by-product, mainly from salt accumulation, which significantly weaken the sensitivity and effectiveness of the polymer, especially, in the pH-responsive MIPs system.[34] In order to eliminate by-product accumulation during pH-responsive processes and meet certain requirements, it is crucial to develop novel stimulating signals with similar functionalities to pH stimulus but without the use of external acids or alkalis.

From the point of view of biocompatibility and toxicity in bio-applications, gas-responsive polymers have been examined as a great substitute for pH-responsive polymers systems, in particular, by using the environmentally-friendly trigger, carbon dioxide (CO_2).[35, 36] CO_2-responsive processes can be automatically tuned by the corresponding phase transition behavior of the polymers from the introduction of CO_2 in an aqueous solution but without any by-product accumulation. For example, Kitayama reported the reversible structural conversion of such samples between born imidazoline functional groups and imidazolinium bicarbonate upon the introduction and removal of CO_2.[37] In addition, polymers containing tertiary amine groups, such as poly(*N,N′*-dimethylaminoethylmethacrylate) (*p*-DMAEMA), are also endowed with CO_2 responsiveness and experience phase transition when CO_2 is induced into the *p*-DMAEMA containing aqueous solution.[38] Such properties make CO_2-responsive polymers widely applied for different domains such as catalysts,[39] separation,[40] CO_2-manipulated drug delivery,[41] CO_2 capturing and monitoring,[42] CO_2-triggered self-assemblies,[43] CO_2-switchable surfaces,[44] and so on. However, it is still rare to combine gas-responsive polymers with molecular imprinting technology, which could offer a useful strategy to realize reversible responsive recognition behavior without any contamination. In this paper, gas-responsive molecularly imprinted hydrogel (GR-MIH) were prepared from a gas switchable monomer, *N,N′*-dimethylaminoethylmethacrylate (DMAEMA). Gas driven reversible conformations of the monomer and polymer were original from the formation of H^+—HCO_3^- by the introduction of CO_2 in an aqueous solution, respectively. This promising process was confirmed by ^1H NMR, SEM and contact angle tests. By applying this property to the sensing application, the novel CO_2-responsive hydrogel

molecularly imprinted towards human serum albumin (HSA) was firstly prepared on the surface of a glassy carbon electrode (GCE) via free radical polymerization. The reversible sensing process towards HSA was achieved by alternatively bubbling with N_2 and CO_2 for HSA removal and imprinting in aqueous solutions, respectively. To the best of our knowledge, this is the first report on the gas-responsive MIH electrochemical biosensor with the gas-responsive self-cleaning property toward the target protein.

2. Experimental Section

2.1 Materials

N,N′-dimethylaminoethyl methacrylate (DMAEMA), *N,N′*-methylenebis(acrylamide) (MBAAm), *N*-isopropylacrylamide (NiPAAm), *N,N,N′,N′*-tetramethylethylenediamine (TEMED), and ammonium persulfate (APS) were purchased from Aladdin Reagents. Human serum albumin (HSA), *α*-fetoprotein (AFP), bovine serum albumin (BSA), human chorionic gonadotropin (HCG), and carcino-embryonic antigen (CEA) were purchased from Shanghai Linc-Bio Science Co. Ltd.

2.2 Apparatus and procedures

CHI660C electrochemical workstation (Chenhua, Shanghai, China) was used to provide measurements in differential pulse voltammetry (DPV), electrochemical impedance spectroscopy (EIS), and cyclic voltammetry (CV). A bare or modified glassy carbon electrode (GCE), a saturated calomel, and a platinum wire were used as the working electrode, reference electrode (SCE), and auxiliary electrode. The gas-sensitive behaviors of DMAEMA monomer were characterized by ^{1}H NMR. The chemical characteristics of gas-responsive MIH film were qualified by Fourier transform infrared spectroscopy (FT-IR) (Bruker, VERTEX 70, Germany). A UV-vis spectrophotometer (Hitachi, UV-3900H, Japan) was used to measure HSA concentrations in serum samples by a standard calibration curve method. The contact angles of the gas-responsive MIH film before and after treated with CO_2 or N_2 were monitored by a contact angle measuring device (Krüss, DSA25, Germany). Each sample was measured with a 2-μL drop of double-distilled water. The surface

morphologies of the gas-responsive MIH film before and after treated with CO_2 or N_2 were monitored by field emission scanning electron micrographs (Hitachi, SU-8220, Japan) with the sample preparation as follows. In particular, the gas-responsive MIH film was initially whipped into a bottle of liquid nitrogen for 5 min to "freeze" the structures, after treated with CO_2 or N_2. Subsequently, a freeze drier (LGJ-18S; Beijing Songyuan Huaxing Technology) was used to dehydrate the obtained frozen film for 24 h.

2.3 Synthesis of gas-responsive imprinted biosensor

The gas-responsive MIH (GR-MIH) electrochemical biosensor was fabricated using the following procedure. Firstly, 300.0 mg of NiPAAm, 30.0 μL of DMAEMA, 5.0 mg of HSA, 5.0 mg MBAAm, 5.0 mg mL^{-1} APS, and 4.0 μL TEMED were dissolved in 1.0 mL double-distilled water to form a pre-imprinting suspension at 0 °C with CO_2 bubbling of 10 min. The DMAEMA will partially decompose and generate methacrylic acid and amino alcohol at 25 °C (Fig. S1†). Therefore, in order to avoid the decomposition of DMAEMA, the preparation of the hydrogel was performed at 0 °C. Then, 6.0 μL of the pre-imprinting solution was drop-casted onto the pre-polished GCE (3 mm) under CO_2 atmosphere at 0 °C. The HSA imprinted hydrogel film was finally formed onto the GCE (HSA imprinted GR-MIH/GCE) under 0 °C after 4 h. For comparison, a GCE modified with gas-responsive non-imprinted hydrogel (GR-NIH/GCE) was processed in the same way with the absence of any templates. Moreover, a none gas-responsive imprinted biosensor was also prepared following the same procedure, while without the addition of DMAEMA (MIH/GCE without DMAEMA).

During this study, HSA was removed from the HSA imprinted GR-MIH/GCE by introducing N_2 for 30 min in water and the round of HSA was performed by introducing CO_2 to a HSA aqueous solution. The details are shown in Scheme 1.

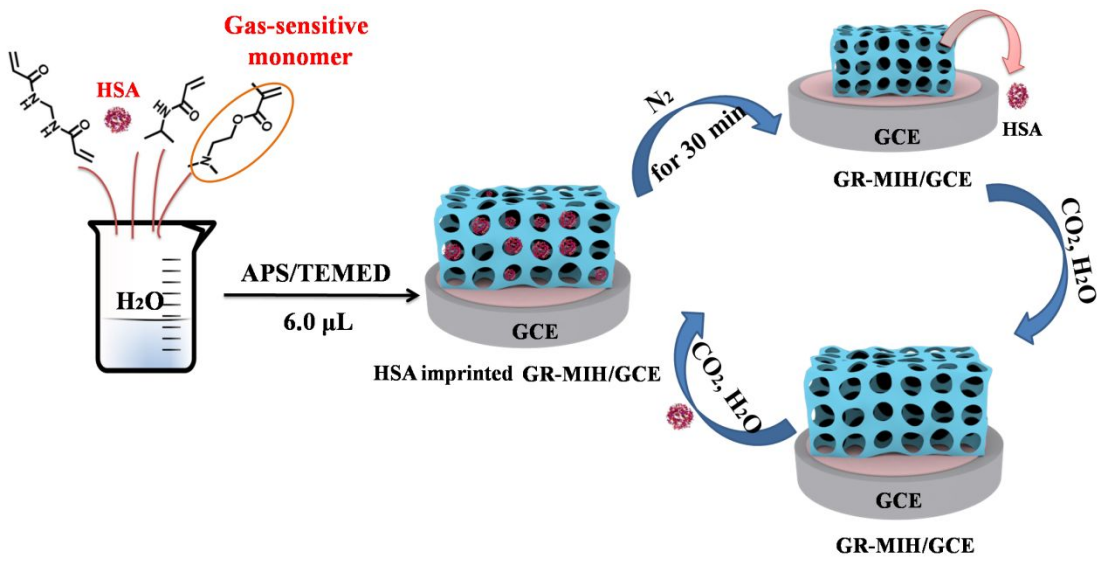

Scheme 1 Schematic illustration of the preparation of gas-responsive HSA imprinted polymers via free radical polymerization, the self-cleaned process of HSA imprinted polymers and re-adsorption process.

3. Results and discussion

3.1 Gas-responsive behavior of DMAEMA monomer

The CO_2-responsive behavior of DMAEMA was successfully demonstrated by ^1H NMR spectra (Fig. 1) at 0 ^oC. The reversible process affected by the change of the tertiary amine group upon bubbling with CO_2 and N_2 in D_2O can be monitored by the field shifts of the protons of methyl (e) and two methylene functional groups (d, c) at 2.26, 2.73-2.70, and 4.29-4.26 ppm. Upon the addition of CO_2 (curve b), these signals spread and shift to lower fields (d=2.89, d=3.47-3.46, and d=4.50-4.48), indicating that the bicarbonate salts of protonated amine groups was formed in this state. By contrast with the introduction of N_2, these signals spread and shift to higher fields (d=2.47, d=2.98-2.95, and d=4.36-4.33). This indicated that the deprotonated amine groups were formed in this state. These observations suggested that tertiary amine groups of DMAEMA can react with bicarbonate generated by the dissolution of CO_2 in an aqueous solution under CO_2 treatment, which leads to the formation of protonation and charged states. The reverse process is realized by purging inert N_2.

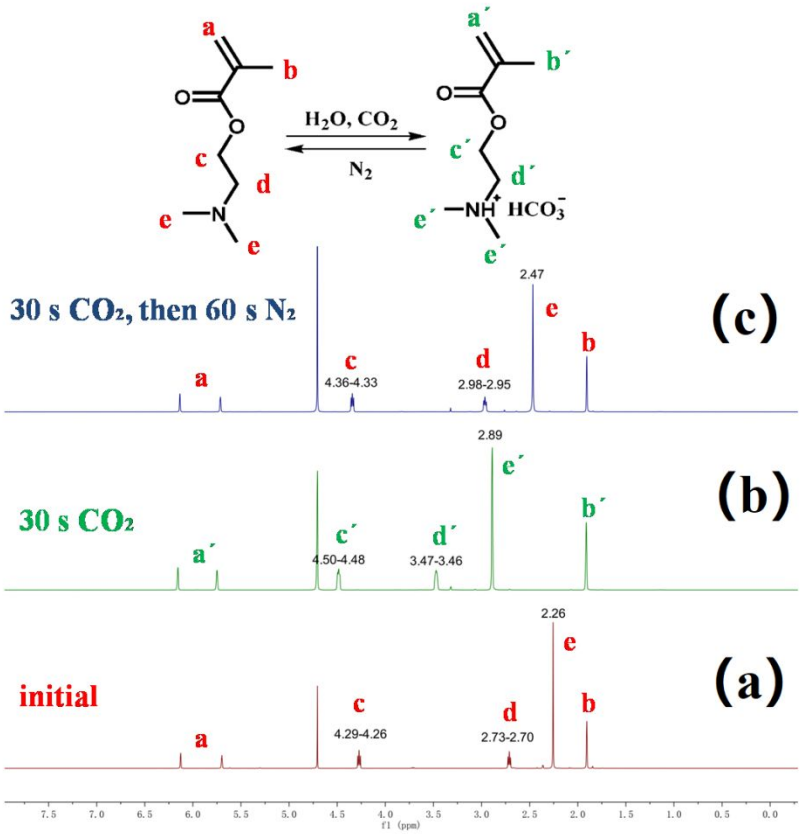

Fig. 1 ^{1}H NMR spectra of DMAEMA monomer (a) in D_2O recorded, (b) which was purged with CO_2 for 30 s, Subsequently (c) N_2 was bubbled again for 60 s at 0 ^{o}C.

3.2 Gas-responsive phase transition of the GR-MIH

As shown in Fig. S2†, the prepared GR-MIH and MIH film without DMAEMA were initially characterized by FT-IR spectra. After polymerization, both gel polymers have the characteristic features assigned to the carbonyl bending vibration of amide group as well as the N-H stretching vibration in the NiPAAm at 1642 cm^{-1}, 1547 cm^{-1} and the region of 3600-3100 cm^{-1}.[45] By contrast, two new bands at 2920 cm^{-1} and 1718 cm^{-1} appear in GR-MIH only. The former is the asymmetrical stretching vibration absorption of C-H bond of the tertiary amine group and the latter is attributed to the bending vibration absorption of C=O stretching vibration of the esters groups.[46] It suggests that DMAEMA is unique in GR-MIH rather than MIH film without DMAEMA.

Furthermore, SEM and contact angle measurements have been applied to reveal the CO_2 and N_2 triggered conformation changes of GR-MIH after five cycles. Upon N_2 treatment, the SEM images show that the GR-MIH film has a surface morphology

of small holes with roughly 3 ± 1 μm pores diameter (Fig. 2A). After treated with CO_2, the structure of film became swollen, with an increase to 6 ± 1 μm (Fig. 2B). Meanwhile, the water-contact angle of the GR-MIH decreased from 54.2° to 17.5° after the CO_2 purge, indicating that GR-MIH turned more hydrophilic. After introducing N_2 to liberate the dissolved CO_2, the pores diameter is almost restored to the original size of 3 ± 1 μm and the contact angle increased back to 51.3° (Fig. 2C and the inset). However, it is not the case for MIH film without DMAEMA (Fig. S3† and the insets), the size and water-contact angle of MIH film is basically unchanged under gas-driven. It is suggested that gas-driven has an obvious effect on the hydrophilicity of GR-MIH film surface. Associated with the results of ^1H NMR spectra, the tertiary amine groups inside sensing nanocavities are in a form of the deprotonated and uncharged state under N_2 atmosphere, obtaining a compact and contracted network structure. After introducing CO_2, most of tertiary amine groups in sensing cavities are interacted with CO_2 dissolved in water, producing bicarbonate salts in their positively charged states. The repulsion interaction between positively charged groups causes the swelling of GR-MIH film on the electrode surface. Subsequently, the structure of GR-MIH film recovered completely after bubbling with N_2 again, because of the liberation of dissolved CO_2 by N_2. This conclusion is also supported by the variation of solution pH. pK_a of *p*-DMAEMA was reported at approximate 7.0. Introduction of CO_2 to the aqueous solution, in which the GR-MIH were immersed, causes a decrease in pH from 7.0 to 5.6. It is mainly due to the formation of carbic acid, which is further converted to the bicarbonate salts with tertiary amine groups in polymers. Reversiblebly, pH of the solution changes from 5.6 back to 7.0, while introducing N_2 to liberate the dissolved CO_2.

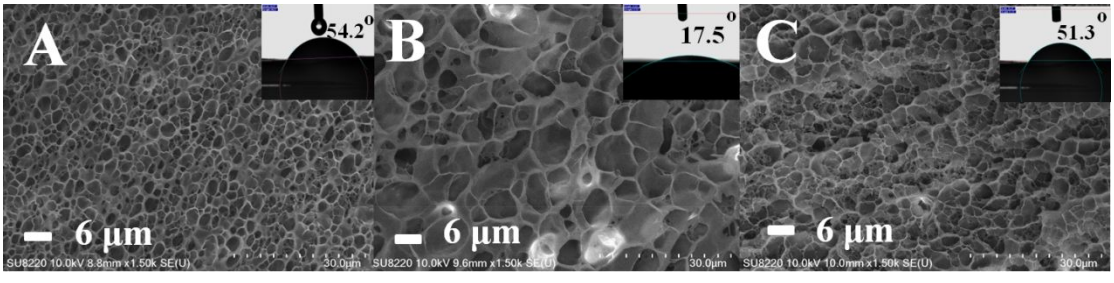

Fig. 2 SEM of the freeze-dried GR-MIH film (A) prepared by plunging from an aqueous solution

saturated with N2, (B) GR-MIH film plunged from a solution which was purged with CO_2 for 20 min, Subsequently N_2 was bubbled again for 30 min in GR-MIH film (C) after five cycles. Insets are the corresponding contact angles of the hydrogel.

3.3 Gas-responsive properties of interfacial GR-MIH/GCE

To investigate the biosensing property of GR-MIH/GCE, we modified the surface of a GCE with HSA imprinted GR-MIH. CVs of $[Fe(CN)_6]^{3-/4-}$ were conducted to validate the formation process of HSA imprinted GR-MIH/GCE and displayed in Fig. S4†. The GR-MIH/GCE exhibits obviously responsiveness on peak currents of the redox probe under the same treatment conditions as GR-NIH/GCE. This result reveals that some cavities were recombined with template and the electron transfer of the redox probe was limited on the electrode surface in the imprinted biosensor. Subsequently, experiments were employed to investigate the gas driven self-clean ability of HSA imprinted GR-MIH/GCE biosensor under N_2 treatment conditions in aqueous solutions at different times (5 min, 10 min, 15 min, 20 min, 30 min, and 40 min) by CV of $[Fe(CN)_6]^{3-/4-}$ at 25 °C (Table S1†). The results indicated that purging with N_2 for 30 min is considered as the optimal condition for the gas-based HSA self-cleaning. As a comparison, the HSA imprinted MIH/GCE without DMAEMA were also investigated under the optimal condition *e.g.* purging with N_2 for 30 min. As shown in Table S1†, there was no significant change observed on currents due to the lack of gas-responsive functional groups in the imprinting processes. Furthermore, the CO_2 responsive behavior of the GR-MIH/GCE was also electrochemically investigated by alternately bubbling with CO_2 and N_2 in the aqueous solution without the standby time. As shown in Fig. 3A, the GR-MIH/GCE exhibited the lowest current signal of $[Fe(CN)_6]^{3-/4-}$ when immersed in the aqueous solution saturated with N_2 for 30 min (Fig. 3A, curve a). After bubbled with CO_2 for 20 min, the current of the redox probe obviously increased (Fig. 3A, curve b). Subsequent, CO_2 in the solution was expelled via bubbling with N_2 for 30 min, which again weakened the CV responses (Fig. 3A, curve c). The variations on $[Fe(CN)_6]^{3-/4-}$ oxidation peak currents from the GR-MIH/GCE are fully reversible upon the gas stimulus ON-OFF switch by respectively introducing CO_2 and N_2 for at least five

cycles (Fig. 3B). Accordingly, the GR-MIH/GCE undergoes a stable gas stimulus ON-OFF switch capability in view of its gas responsive property, and exhibits a cavities volume changes (from an extended structure to collapsed structure) with repeatable bubbling the solution with CO_2 and N_2, respectively. The results of CVs coincide with observation on EIS (Fig. 3C), where the $[Fe(CN)_6]^{3-/4-}$ charge transfer ability to the GCE surface can be shown by the interfacial electron transfer resistance (ETR) and relied on bubbling with CO_2 and N_2, respectively. The result gave strong evidence for the conversion of the eternal gas-stimulus signals directly into an electrochemical response by the GR-MIH/GCE interfaces with a quick electrochemical switching ability and reversible cyclicity. As verified by SEM images of freeze-dried GR-MIH, these observations are the results of the transition between the deprotonated and protonated states of DMAEMA chains in the GR-MIH.

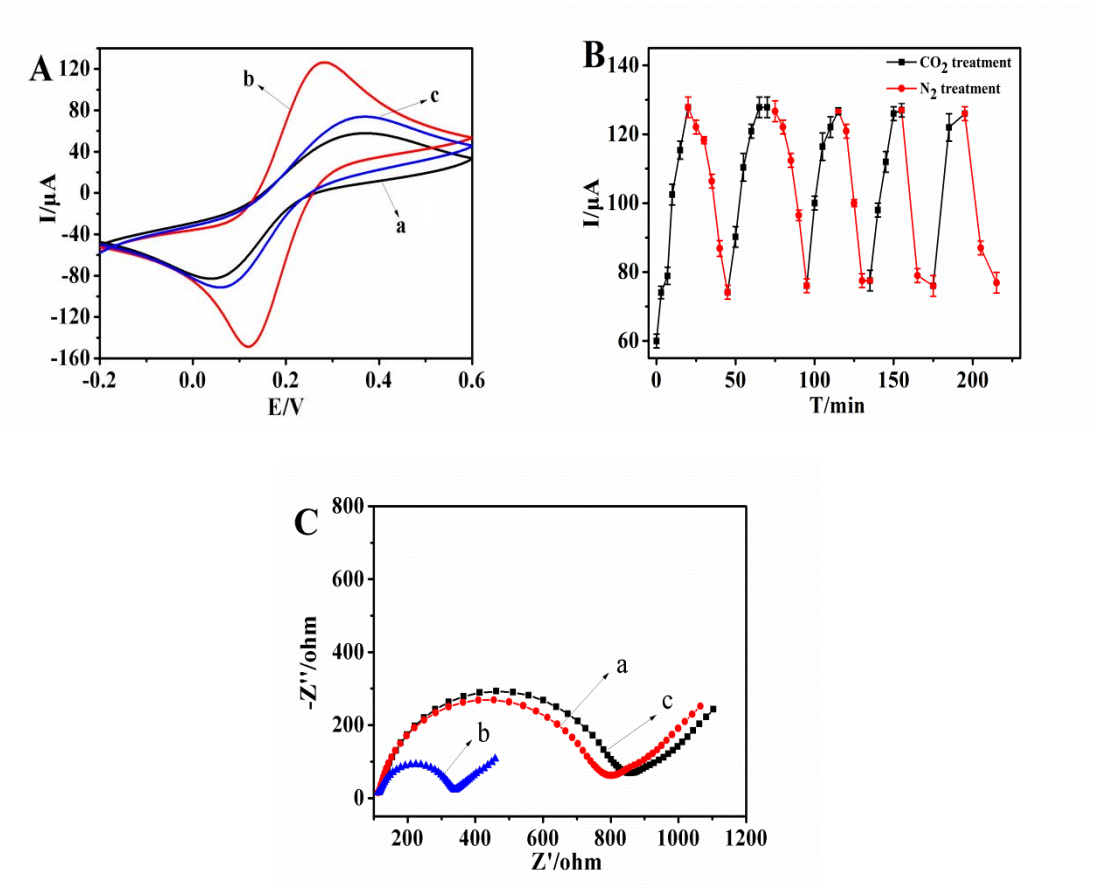

Fig. 3 (A) CV responses of GR-MIH/GCE in aqueous solution of saturated with N_2 (curve a), after CO_2 was bubbled for 20 min (curve b), and then N_2 was bubbled again for 30 min (curve c); (B) Variation of CV peak current of the GR-MIH/GCE for the gas stimulus ON-OFF switch between

CO_2 and N_2 in aqueous solution for five cycles; (C) EIS responses of GR-MIH/GCE in aqueous solution of saturated with N_2 (curve a), after CO_2 was bubbled for 20 min (curve b), and then N_2 was bubbled again for 30 min (curve c) at frequencies from 0.01 to 10^5 Hz.

3.4 Gas-driven biosensing for HSA by GR-MIH/GCE

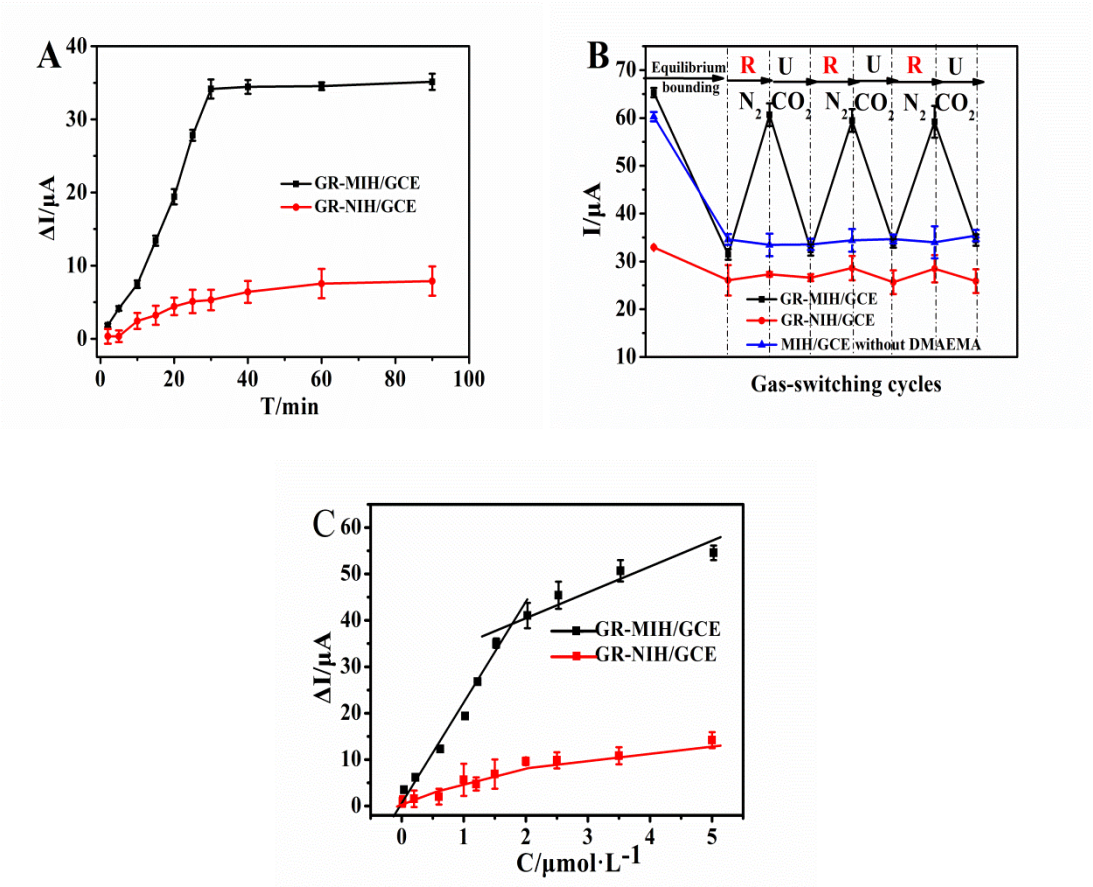

Fig. 4 (A) Adsorption time on the *ΔI* of redox probe for the GR-MIH/GCE and GR-NIH/GCE in 0.5 mL of 1.5 μmol L^{-1} HSA in aqueous solution of saturated with CO_2 at 25 °C; (B) Gas-driven release (R) and uptake (U) of 1.5 μmol L^{-1} HSA on the peak current of redox probe by alternately bubbling with N_2 and CO_2 for three cycles using the GR-MIH/GCE, GR-NIH/GCE, and MIH/GCE without DMAEMA; (C) Calibration curves of the GR-MIH/GCE and GR-NIH/GCE toward HSA standards in aqueous solution of saturated with CO_2 at 25 °C.

The incubation time is one of the most important parameters for evaluating the behavior of GR-MIH/GCE biosensor. Fig. 4A illustrates the variation of the DPV peak current (*ΔI*) from the GR-MIH/GCE and GR-NIH/GCE biosensor in case of adsorption time in an aqueous solution saturated with CO_2. It can be seen that *ΔI* of the redox probe was dramatically increased and attained a stable situation when the

GR-MIH/GCE biosensor was interacted with HSA under the CO_2-treated condition. However, for the GR-NIH/GCE (curve c), the adsorption was evidently lower than that of GR-MIH/GCE, owing to lacking of recognition sites.

To this end, we explored the adsorption characteristics under N_2 and CO_2 cycles. The GR-MIH/GCE can perform efficiently of releasing and uptaking HSA under alternating N_2 and CO_2 treatments. For the GR-MIH/GCE, the DPV peak current of the redox probe was 31 μA when the adsorption of HSA was achieved in equilibrium in the aqueous solution saturated with CO_2, as shown in Fig. 4B. The recognition sites and micropore size of sensing cavities are complementary to the HSA at utmost at this point. Afterwards, N_2 was bubbled to the HSA imprinted GR-MIH/GCE. It leads to the increase of DPV peak current, owing to releasing the re-bound HSA into the solution because of the conversion from charged bicarbonate salts of tertiary amines to their deprotonated and uncharged states inside nanocavities.

As a consequence, the attractive interaction (the electrostatic and hydrogen bonding forces) between the functional monomers and HSA is decreased and the protein is released. Hence, the gas-responsive rebinding capacity mainly originates from the gas-dependent volume phase transition as well as from the two states of tertiary amine groups part in *p*-DMAEMA of the GR-MIH. For the use of a large amount of NiPAAm, the function of the role lies in the hydrogel construction. During the procedure, the imprinted biosensor exhibited good electrochemical stability and reversibility. For the non-imprinted biosensor, an ignorable current change was detected after three cycles in similar steps. However, the MIH/GCE without DMAEMA lacks of gas-responsive functional groups in the structure and is not able to undergo the imprinting process to release HSA, reflecting the negligible changes in current under the same conditions.

The binding isotherms of HSA by the GR-MIH/GCE under CO_2 treatment condition have also been studies by DPV of the redox probe. The GR-MIH/GCE exhibits two linear calibration curves with lower and higher concentrations (Fig. 4C). Namely, ΔI (μA) = 0.0468 + 18.67$C_{[HSA]}$ (R^2 = 0.98) (0.015-1.5 μmol L^{-1}) and ΔI (μA) = 25.76 + 5.96$C_{[HSA]}$ (R^2 = 0.94) (1.5-5.0 μmol L^{-1}), respectively, with a favorable

detection limit of 0.016 μmol L^{-1}, which indicates that two kinds of affinity sites at high and low exist in the GR-MIH/GCE. By contrast, the GR-NIH/GCE does not respond to the HSA and the obtained ΔI is negligible, owing to lacking of binding sites in the structure of GR-NIH/GCE. To further assess the binding isotherms of the GR-MIH/GCE under CO_2 treatment, the application of Scatchard plot to fit these static adsorption data has been shown in Fig. S5†. The plot exhibits two linear components with different slopes. These observations are correlated with the specific recognition sites and non-specific recognition sites toward HSA contained in the imprinted biosensor. The values of specific binding constant k_d and binding density Q_{max} have been determined as 1.175 mol L^{-1} and 0.781 mmol L^{-1}, respectively and k_d is calculated from the slope of the template specific binding line (in Fig. S4†) using origin software (slope=-1/k_d). Target species could easily diffuse into the recognition sites of GR-MIH/GCE, thus leading to high binding capacity and fast mass-transfer rate. For GR-NIH/GCE, no tailor-made recognition sites have been found, and the template molecules adsorbed on GR-NIH/GCE are far less than those on GR-MIH/GCE due to the absence of reorganization sites.

A selectivity experiment was carried out, using the selected potential interferents, including HSA (MW 66 kDa), BSA (MW 66 kDa), AFP (MW 70 kDa), HCG (MW 36 kDa), and CEA (MW 180 kDa) to the assessment of the GR-MIH/GCE selectivity (Fig. S6). By DPV, the ΔI of redox probe on GR-MIH/GCE toward HSA is higher than the other analogues. For control, the GR-NIH/GCE toward HSA can scarcely be distinguished from analogues, due to lacking of template cavities. The obtained results well prove that this method is reasonable and feasible. Besides, after the preservation of the GR-MIH/GCE biosensor at 4 °C for 5 days, nearly 89% of the initial peak current was obtained. The obtained results well prove that this method is reasonable and feasible. The applicability of the obtained GR-MIH/GCE was achieved by extracting HSA from serum samples. The serum samples were collected from a healthy volunteer and disposed by the methods from literature. As summarized in Table S2†, the GR-MIH/GCE was able to extract HSA from serum samples with excellent recoveries varied between 92.5% and 112.1% for six measurements, which

was determined by the UV–vis spectroscopic method.[47] We also compared the performances of GR-MIH/GCE biosensor with other reported HSA electrochemical imprinted biosensors. Table S3† exhibits the GR-MIH/GCE biosensor possessing the range of wide linear dynamic and an acceptable limit of detection.

4. Conclusions

GR-MIH possessing HSA extraction ability was successfully fabricated using free radical polymerization method with immobilization of HSA in specific conformations on the surface of GCE via hydrogen bonding and electrostatic force. In this design, the tertiary amine groups were left inside the imprinted cavities that are capable of releasing and uptaking HSA under alternately bubbling N_2 and CO_2. The obtained biosensor showed higher affinity under CO_2 treatment condition than that of N_2 treatment, verifying the efficiency of the gas controlled imprinting process. Enlightened by these, the biosensor has the functionality of gas-based cleaning to the HSA without the help of washing solvents. It is not reported by other HSA imprinted biosensors literatures. Besides, the GR-MIH/GCE biosensor is not just as an effective and reliable biosensing platform towards HSA. It also provides gas-driven extraction function. The results indicate that the GR-MIH/GCE biosensor are endowed with highly effective, precise and it is potentially applications for detecting and extracting HSA from serum samples.

Acknowledgements

This work was financially supported by the National Natural Science Foundation of China (Grant Nos. 21475046, 21427809, 21874047).

References

(1) Wei, Y.; Zeng, Q.; Hu, Q.; Wang, M.; Tao, J.; Wang, L. Self-Cleaned Electrochemical Protein Imprinting Biosensor basing on a Thermo-Responsive Memory Hydrogel. *Biosens. Bioelectron.* **2018**, 99, 136-141.

(2) Lyon, L. A.; Meng, Z.; Singh, N.; Sorrell, C. D.; John, A. S. Thermoresponsive Microgel-Based Materials. *Chem. Soc. Rev.* **2009**, 38, 865-874.

(3) Yang, H.; Zhu, H.; Hendrix, M. M.; Lousberg, N. J.; de With, G.; Esteves, A. C.; Xin, J. H. Temperature-Triggered Collection and Release of Water from Fogs by a Sponge-Like Cotton

Fabric. *Adv. Mater.* **2013**, 25, 1150-1154.

(4) Zhong, Q.; Chen, Y. Y.; Guan, S. L.; Fang, Q. S.; Chen, T.; Müller-Buschbaum, P.; Wang, J. P. Smart Cleaning Cotton Fabrics Cross-linked with Thermo-Responsive and Flexible Poly(2-(2-methoxyethoxy)ethoxyethyl methacrylate-coethylene glycol methacrylate). *RSC Adv.* **2015**, 5, 38382-38390.

(5) Chen, Y.; An, J.; Zhong, Q.; Müller-Buschbaum, P.; Wang, J. Smart Control of Cotton Fabric Comfort by Cross-Linking Thermo-Responsive Poly(2-(2-methoxyethoxy) ethoxyethyl methacrylate-co-ethylene glycol methacrylate). *Text. Res. J.* **2017**, 87, 1620-1630.

(6) Hu, J.; Zhang, G.; Liu, S. Enzyme-Responsive Polymeric Assemblies, Nanoparticles and Hydrogels. *Chem. Soc. Rev.* **2012**, 41, 5933-5949.

(7) Yu, L.; Cheng, M.; Song, M.; Zhang, D.; Xiao, M.; Shi, F. pH-Responsive Round-Way Motions of a Smart Device Through Integrating Two Types of Chemical Actuators in One Smart System. *Adv. Funct. Mater.* **2015**, 25, 5786-5793.

(8) Wei, Y.; Zeng, Q.; Bai, S.; Wang, M.; Wang, L. Nanosized Difunctional Photo Responsive Magnetic Imprinting Polymer for Electrochemically Monitored Light-Driven Paracetamol Extraction. *ACS Appl. Mater. Interfaces* **2017**, 9, 44114-44123.

(9) Gong, C.-B.; Wei, Y.-B.; Liu, L.-T.; Zheng, A.-X.; Yang, Y.-H.; Chow, C.-f.; Tang, Q. Photoresponsive Hollow Molecularly Imprinted Polymer for Trace Triamterene in Biological Samples. *Mater. Sci. Eng. C* **2017**, 76, 568-578.

(10) Gong, C.-b.; Wei, Y.-b.; Chen, M.-j.; Liu, L.-t.; Chow, C.-f.; Tang, Q. Double Imprinted Photoresponsive Polymer for Simultaneous Detection of Phthalate Esters in Plastics. *Eur. Polym. J.* **2018,** 108, 295-303.

(11) Zhong, Q.; Lu, M.; Nieuwenhuis, S.; Wu, B. S.; Wu, G. P.; Xu, Z. K.; Müller-Buschbaum, P.; Wang, J. P. Enhanced Stain Removal and Comfort Control Achieved by CrossLinking Light and Thermo Dual-Responsive Copolymer onto Cotton Fabrics. *ACS Appl. Mater. Interfaces* **2019**, 11, 5414-5426.

(12) Hosseini-Nassab, N.; Samanta, D.; Abdolazimi, Y.; Annes, J. P.; Zare, R. N. Electrically Controlled Release of Insulin using Polypyrrole Nanoparticles. *Nanoscale* **2017,** 9, 143-149.

(13) Zamora-Gálvez, A.; Ait-Lahcen, A. L.; Mercante, A.; Morales-Narváez, E.; Amine, A.; Merkoçi, A. Molecularly Imprinted Polymer-Decorated Magnetite Nanoparticles for Selective

Sulfonamide Detection. *Anal. Chem.* **2016**, 88, 3578-3584.

(14) Williams, R. J.; Smith, A. M.; Collins, R.; Hodson, N.; Das, A. K.; Ulijin, R. V. Enzyme-assisted Self-assembly under Thermodynamic Control. *Nat. Nanotechnol.* **2009**, 4, 19-24.

(15) Wei, Y.-b.; Tang, Q.; Gong, C.-b.; Lam, M. H.-W. Review of the Recent Progress in Photoresponsive Molecularly Imprinted Polymers Containing Azobenzene Chromophores. *Anal. Chim. Acta* **2015,** 900, 10-20.

(16) Hu, J.; Meng, H.; Li, G.; Ibekwe, S. I. A Review of Stimuli-Responsive Polymers for Smart Textile Applications. *Smart Mater. Struct.* **2012**, 21, 53001-53023.

(17) Paek, K.; Yang, H.; Lee, J.; Park, J.; Kim, B. J. Efficient Colorimetric pH Sensor Based on Responsive Polymer Quantum Dot Integrated Graphene Oxide. *ACS Nano* **2014,** 8, 2848-2856.

(18) Li, Z.-y.; Quan, H.-j.; Gong, C.-b.; Yang, Y.-z.; Tang, Q.; Wei, Y.-b.; Ma, X.-b.; Lam, H.-w. Photocontrolled Solid-phase Extraction of Guanine from Complex Samples Using a Novel Photoresponsive Molecularly Imprinted Polymer. *Food Chem.* **2015,** 172, 56-62.

(19) Hong, B. J.; Chiper, A. J.; Nguyen, S. T. Macromolecular Amplification of Binding Response in Superaptamer Hydrogels. *J. Am. Chem. Soc.* **2013**, 135, 17655-17658.

(20) Wang, J.; Chen, Y.; An, J.; Xu, K.; Chen, T., Müller-Buschbaum, P.; Zhong, Q. Intelligent Textiles with Comfort Regulation and Inhibition of Bacterial Adhesion Realized by Cross-Linking Poly(n-isopropylacrylamide-co-ethylene glycol methacrylate) to Cotton Fabrics. *ACS Appl. Mater. Interfaces* **2017**, 9, 13647-13656.

(21) Ran, D.; Wang, Y.; Jia, X.; Nie, C. Bovine Serum Albumin Recognition via Thermosensitive Molecular Imprinted Macroporous Hydrogels Prepared at Two Different Temperatures. *Anal. Chim. Acta* **2012**, 723, 45-53.

(22) Bakhshpour, M.; Özgür, E.; Bereli, N.; Denizli, A. Microcontact Imprinted Quartz Crystal Microbalance Nanosensor for Protein C Recognition. *Colloids Surf. B* **2017**, 151, 264-270.

(23) Pan, G.; Guo, Q.; Ma, Y.; Yang, H.; Li, B. Thermo-Responsive Hydrogel Layers Imprinted with RGDS Peptide: A System for Harvesting Cell Sheets. *Angew. Chem. Int. Ed.* **2013**, 52, 6907-6911.

(24) Pan, J.; Chen, W.; Ma, Y.; Pan, G. Molecularly Imprinted Polymers as Receptor Mimics for Selective Cell Recognition. *Chem. Soc. Rev.* **2018,** 47, 5574-5587.

(25) Zadok, I.; Srebnik, S. Coarse-Grained Simulation of Protein-Imprinted Hydrogels. *J. Phys.*

Chem. B **2018**, 122, 7091-7101.

(26) Chen, L.; Wang, X.; Lu, W.; Wu, X.; Li, J. Molecular Imprinting: Perspectives and Applications. *Chem. Soc. Rev.* **2016**, 45, 2137-2211.

(27) Li, S.; Cao, S.; Whitcombe, M. J.; Piletsky, S. A. Size Matters: Challenges in Imprinting Macromolecules. *Prog. Polym. Sci.* **2014**, 39, 145-163.

(28) Wulff, G. Fourty Years of Molecular Imprinting in Synthetic Polymers: Origin, Features and Perspectives. *Microchim. Acta* **2013**, 180, 1359-1370.

(29) Wei, Y.; Zeng, Q.; Huang, J.; Hu, Q.; Guo, X.; Wang, L. An Electro-Responsive Imprinted Biosensor with Switchable Affinity toward Proteins. *Chem. Commun.* **2018**, 54, 9163-9166.

(30) Kocak, G.; Tuncer, C.; Bütün, V. pH-Responsive Polymers. *Polym. Chem.* **2017**, 8, 144-176.

(31) Hu, J.; Zhang, G.; Ge, Z.; Liu, S. Stimuli-Responsive Tertiary Amine Methacrylate-Based Block Copolymers: Synthesis, Supramolecular Self-Assembly and Functional Applications. *Prog. Polym. Sci.* **2014**, 39, 1096-1143.

(32) Hoffman, A. S. Hydrogels for Biomedical Applications. *Adv. Drug Delivery Rev.* **2012**, 64, 18-23.

(33) Dai, S.; Ravi, P.; Tam, K. C. pH-Responsive Polymers: Synthesis, Properties and Applications. *Soft Matter* **2008**, 4, 435-449.

(34) Sun, H.; Chen, X.; Han, X.; Liu, H. Dual Thermoresponsive Aggregation of Schizophrenic PDMAEMA-b-PSBMA Copolymer with an Unrepeatable pH Response and a Recycled CO_2/N_2 Response. *Langmuir* **2017**, 33, 2646-2654.

(35) Liu, H.; Lin, S.; Feng, Y.; Theato, P. CO_2-Responsive Polymer Materials. *Polym. Chem.* **2017**, 8, 12-23.

(36) Yan, Q.; Zhao, Y. Block Copolymer Self-Assembly Controlled by the "Green'' Gas Stimulus of Carbon Dioxide. *Chem. Commun.* **2014**, 50, 11631-11641.

(37) Kitayama, Y.; Isomura, M. Gas-Stimuli-Responsive Molecularly Imprinted Polymer Particles with Switchable Affinity for Target Protein. *Chem. Commun.* **2018**, 54, 2538-2541.

(38) Darabi, A.; Jessop, P. G.; Cunningham, M. F. CO_2-Responsive Polymeric Materials: Synthesis, Self-Assembly, and Functional Applications *Chem. Soc. Rev.* **2016**, 45, 4391-4436.

(39) Zhang, J.; Han, D.; Zhang, H.; Chaker, M.; Zhao, Y.; Ma, D. In Situ Recyclable Gold Nanoparticles using CO_2-Switchable Polymers for Catalytic Reduction of 4-Nitrophenol. *Chem.*

Commun. **2012**, 48, 11510-11512.

(40) Yu, G.; Lu, Y.; Liu, X.; Wang, W.-J.; Yang, Q.; Xing, H.; Ren, Q.; Li, B.-G.; Zhu, S. Polyethylenimine-Assisted Extraction of α-Tocopherol from Tocopherol Homologues and CO_2-Triggered Fast Recovery of the Extractant. *Ind. Eng. Chem. Res.* **2014**, 53, 16025-16032.

(41) Che, N.; Yang, S.; Kang, H.; Liu, R.; Li, Z.; Liu, Z.; Li, P.; Qu, X.; Huang, Y. Synthesis and Properties of CO_2-Switchable Dex-g-PAHMA Copolymers. *Polym. Chem.* **2014**, 5, 7109-7120.

(42) Xu, L. Q.; Zhang, B.; Sun, M.; Hong, L.; Neoh, K.-G.; Kang, E.-T.; Fu, G. D. CO_2-Triggered Fluorescence "Turn-On" Response of Perylene Diimide-Containing poly(N,Ndimethylaminoethyl methacrylate). *J. Mater. Chem. A* **2013**, 1, 1207-1212.

(43) Yan, Q.; Wang, J.; Yin, Y.; Yuan, J. Breathing Polymersomes: CO_2-Tuning Membrane Permeability for Size-Selective Release, Separation, and Reaction. *Angew. Chem., Int. Ed.* **2013**, 52, 5070-5073.

(44) Kumar, S.; Tong, X.; Dory, Y. L.; Lepage, M.; Zhao, Y. A CO_2-Switchable Polymer Brush for Reversible Capture and Release of Proteins. *Chem. Commun.* **2013**, 49, 90-92.

(45) Liu, G.; Wang, D.; Zhou, F.; Liu, W. Electrostatic Self-Assembly of Au Nanoparticles onto Thermosensitive Magnetic Core-Shell Microgels for Thermally Tunable and Magnetically Recyclable Catalysis. *Small* **2015**, 11, 2807-2816.

(46) Golub, D.; Krajnc, P. Emulsion Templated Hydrophilic Polymethacrylates. Morphological features, Water and Dye Absorption. *React. Funct. Polymer.* **2020**, 149, 104515.

(47) Liu, M.; Pi, J.; Wang, X.; Huang, R.; Du, Y.; Yu, X.; Tan, W.; Liu, F.; Shea, K. J. A Sol-Gel Derived pH-Responsive Bovine Serum Albumin Molecularly Imprinted Poly(ionic liquids) on the Surface of Multiwall Carbon Nanotubes. *Anal. Chim. Acta* **2016**, 932, 29-40

TOC

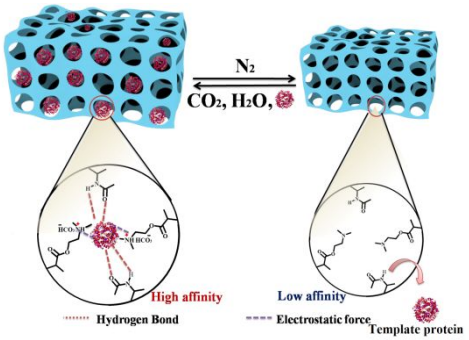
N2
CO2, H2O,
High affinity
Low affinity
Hydrogen Bond
Electrostatic force
Template protein